Title
SIMULATION OF EFFECTS OF REDOX AND PRECIPITATION ON DIFFUSION OF URANIUM SOLUTION SPECIES IN BACKFILL

Author
Carnahan, C.L.

Publication Date
1987-12-01

Lawrence Berkeley Laboratory
UNIVERSITY OF CALIFORNIA

EARTH SCIENCES DIVISION

Presented at the Fall Meeting of the Materials Research Society, Symposium P: Scientific Basis for Nuclear Waste Management XI, Boston, MA, November 30–December 3, 1987, and to be published in the Proceedings

Simulation of Effects of Redox and Precipitation on Diffusion of Uranium Solution Species in Backfill

C.L. Carnahan

December 1987

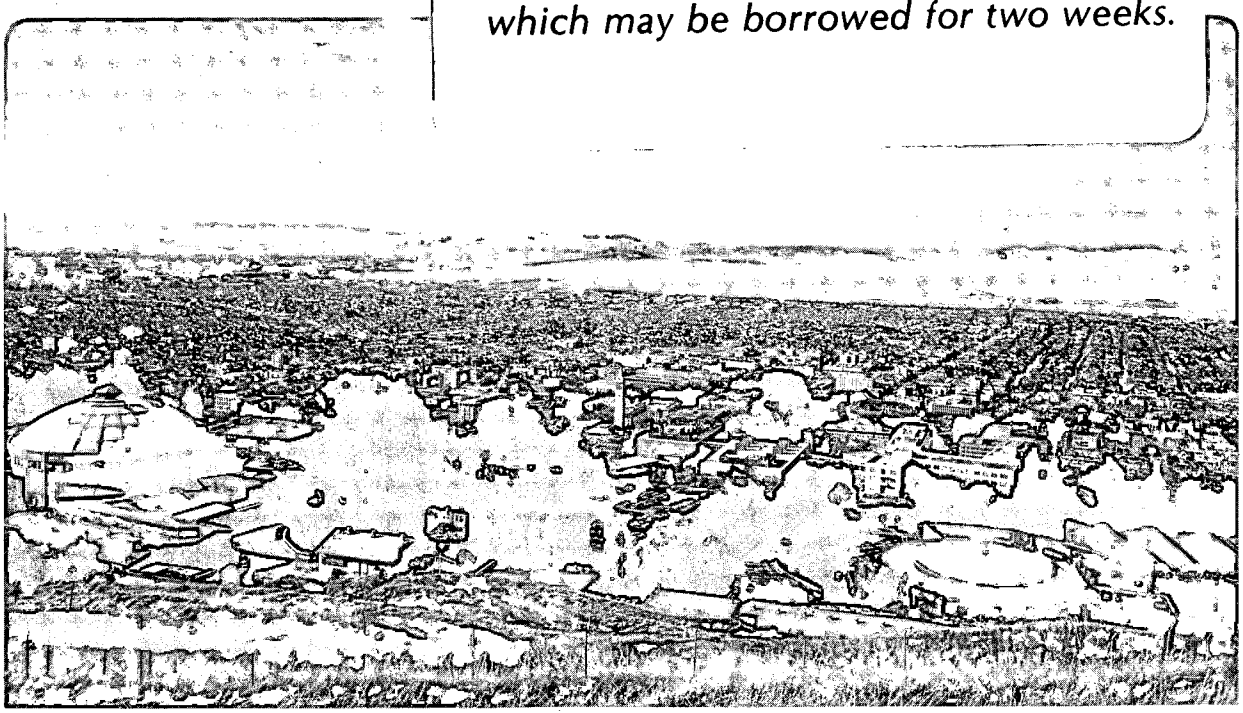

Prepared for the U.S. Department of Energy under Contract DE-AC03-76SF00098

DISCLAIMER

SIMULATION OF EFFECTS OF REDOX AND PRECIPITATION ON DIFFUSION OF URANIUM SOLUTION SPECIES IN BACKFILL

C. L. CARNAHAN
Earth Sciences Division, MS 50E, Lawrence Berkeley Laboratory, University of California, Berkeley, CA 94720.

ABSTRACT

This investigation addresses the problem of prediction of the rate of migration of redox-sensitive solution species within packing and backfill materials under conditions of variable oxidation potential. Effects of changes of oxidation potential and precipitation of stable uranium compounds during diffusion of uranium from a region of high oxidation potential into a region of low oxidation potential were simulated numerically. Questions of particular interest addressed in the investigation were the existence of a moving "redox front" and the influence of precipitation-dissolution processes on uranium migration. The simulations showed that no expanding redox fronts existed at any simulated time up to 3.2×10^5 years (10^{13} s). In simulations where precipitation of stable solids was not allowed, variations of oxidation potential did not affect total uranium concentrations in solution. Concentration profiles could be predicted simply by diffusion of the (constant) source concentrations. In simulations where precipitation of stable solids was allowed, uraninite and calcium uranate accumulated at the source-transport domain interface, while coffinite penetrated further into the transport domain. Total uranium concentrations in regions of precipitation were determined by solubilities of the precipitated solids, and were six to seven orders of magnitude lower than those in the simulations without precipitation, throughout the domain of transport.

INTRODUCTION

The recent literature contains accounts of studies, both theoretical and experimental, of the possibility that dissolution of uranium dioxide may be enhanced by the action of oxidants arising from the presence of oxygen gas or from radiolysis of water.

- A theoretical study [1] simulated the movement of an oxidizing zone, arising from alpha radiolysis, by flowing groundwater into a reducing environment in fractured host rock. The study concluded that the oxidizing zone would not extend more than a few tens of meters from its source region after a million years.
- An experimental study [2] used products of alpha radiolysis of water to investigate oxidation of UO_2; it was found that the rate of oxidation by H_2O_2 is about 200 times faster than by dissolved O_2. In a later study by the same group [3] it was found that the presence of reductants [H_2, Fe(II)] lowered the corrosion potential of UO_2 in the presence of alpha radiation.
- Results of an experimental study [4] suggested that, in basaltic and granitic ground waters containing abundant Fe(II) species, gamma radiolysis may not produce oxidizing conditions.

These studies all are related to the important problem of the prediction of the rate of migration of redox-sensitive solution species within packing and backfill materials under conditions of variable oxidation potential.

In the case of uranium (and other actinides), the total concentration of the element in solution is strongly dependent on oxidation potential. In general, compounds of uranium(VI) are more soluble than uranium(IV) dioxide and their solubility is further enhanced by the formation of complexes with ligands such as the carbonate ion. In basalt

and granite repositories where reducing conditions are expected to prevail initially [5], the existence of an expanding zone of high oxidation potential would mobilize concentrations of dissolved uranium much higher than the concentrations predicted on the basis of the lower oxidation potential. Migration of the relatively high concentrations of uranium could be retarded, however, by precipitation (followed by redissolution) of stable compounds of uranium at the interface between the zones of low and high oxidation potential. Simulation of such a process in flowing groundwater has been described previously [6].

The present investigation focuses on effects of changes of oxidation potential and precipitation of stable uranium compounds during *diffusion* of dissolved uranium from a region with a high oxidation potential into a region with a low oxidation potential. Questions of particular interest addressed in the investigation are the existence of an expanding zone of high oxidation potential (a moving redox front) and the influence of precipitation-dissolution processes on uranium migration.

NUMERICAL SIMULATIONS

The numerical simulations of uranium migration were done by the reactive chemical equilibrium transport program THCC [6], assuming radial diffusion from a constant-concentration source into a semi-infinite, saturated porous medium.

Computer Program THCC

The THCC computer program [6] is a thermodynamically based simulator of multicomponent, reactive chemical transport using the direct method of solution. The program simulates transport of reactive chemical species by advection with constant pore fluid velocity and by hydrodynamic dispersion or chemical diffusion in one-dimensional or cylindrically symmetric geometry. Chemical reactions are assumed to be in a state of local equilibrium. The types of reactions simulated are complexation, oxidation-reduction, and ionization of water in the aqueous phase and reversible precipitation of solid phases. Chemical reactions are described by mass action relations among thermodynamic activities of participating species. Oxidation-reduction reactions are treated by defining a hypothetical electron activity as a basis species subject to transport as are other aqueous basis species. The THCC program has the capability to simulate systems with temporally and spatially variable fields of temperature, although this capability was not used in the simulations reported here.

Basis of Simulations

The simulations assumed that chemical species in a cylindrical source region with an outer radius of 0.5 m diffused radially into a semi-infinite porous medium saturated with a fluid having an initial chemical composition similar to that of a basaltic ground water [5]. The source region had an Eh of +0.3 v in accordance with measured values of oxidation potentials arising from alpha radiolysis [2], and the pH of the source region was 7. Uranium(IV) dioxide is thermodynamically unstable under these conditions, and the solubility of uranium was determined by the equilibria between the stable solid schoepite [$UO_2(OH)_2 \cdot H_2O$(c)] and uranium(VI) solution species including carbonato complexes. Thus, the total uranium concentration in the source region was about 1×10^{-3} M. The fluid occupying the spatial domain was strongly reducing with an Eh of -0.36 v, and its pH was 9.7 [5]. The simulations assumed that this domain had a diffusion coefficient of 1×10^{-10} m^2/s. The temperature of the source region and of the spatial domain was assumed constant at 25 °C. Preliminary calculations with the program THCC showed that

the most significant complexes of uranium(VI) in the source region were $UO_2(CO_3)_2^{2-}$ and $(UO_2)_2(OH)_3CO_3^-$. The only uranium(IV) solution species simulated was $U(OH)_4^0$. Equilibrium compositions of the source and ambient solutions, including both basis species and complexes, are listed in Table I.

Table I. Compositions of source and ambient solutions

Component	Source	Ambient
Na^+	1.60×10^{-2} M	1.60×10^{-2} M
Ca^{2+}	0.	7.00×10^{-5} M
Cl^-	1.52×10^{-2} M	1.49×10^{-2} M
$Si(OH)_4^0$	0.	1.10×10^{-4} M
CO_3^{2-}	2.45×10^{-7} M	2.46×10^{-4} M
HCO_3^-	3.27×10^{-4} M	6.53×10^{-4} M
$H_2CO_3^0$	5.85×10^{-5} M	2.33×10^{-7} M
UO_2^{2+}	3.07×10^{-9} M	0.
$UO_2(CO_3)_2^{2-}$	9.28×10^{-6} M	0.
$(UO_2)_2(OH)_3CO_3^-$	4.95×10^{-4} M	0.
$U(OH)_4^0$	3.39×10^{-15} M	0.
pH	7.0	9.7
Eh	+0.30 v	−0.36 v

Solution species from the source region were allowed to diffuse radially into the spatial domain. Within this domain, precipitation of the following solids was considered: schoepite, uraninite [UO_2(c)], coffinite [$USiO_4$(c)], calcium uranate [$CaUO_4$(c)], and uranophane [$Ca(UO_2)_2(SiO_3OH)_2$(c)]. Simulations were done with and without inclusion of precipitation in the domain of transport. The maximum simulated time was 10^{13} s (3.2×10^5 years). Table II shows the chemical reactions used in the simulations, the common logarithm of the thermodynamic equilibrium constant (K) for each reaction, and the sources of data used to calculate the $\log K$ values. In the absence of a critically evaluated, comprehensive data base for uranium, data from existing compilations were supplemented by more recently published data where available. The questionable species $U(OH)_5^-$ was excluded from the simulations. Thus, the chemical behaviors simulated in this work are based on the assumption of a particular set of thermochemical data [7–12]. However, replacement of any of the data used here by other data extant in the literature could have produced different results for both concentrations of species in solution, times of initial appearance of precipitated solids, and quantities of solids [13].

Table II. Chemical reactions and $\log K$ values used in the simulations

Reaction	$\log K$	Source
$H_2O = H^+ + OH^-$	−13.99	[7]
$H^+ + CO_3^{2-} = HCO_3^-$	10.34	[7]
$2H^+ + CO_3^{2-} = H_2CO_3^0$	16.70	[7]
$UO_2^{2+} + 2CO_3^{2-} = UO_2(CO_3)_2^{2-}$	17.13	[7]
$2UO_2^{2+} + CO_3^{2-} + 3H_2O = (UO_2)_2(OH)_3CO_3^- + 3H^+$	−0.24	[8]
$UO_2^{2+} + 2e^- + 2H_2O = U(OH)_4^0$	4.40	[9,10]
$UO_2(c) = UO_2^{2+} + 2e^-$	−9.99	[9,10]
$UO_2(OH)_2 \cdot H_2O(c) + 2H^+ = UO_2^{2+} + 3H_2O$	5.40	[11]
$USiO_4(c) + 2H_2O = UO_2^{2+} + Si(OH)_4^0 + 2e^-$	−18.54	[11]
$CaUO_4(c) + 4H^+ = UO_2^{2+} + Ca^{2+} + 2H_2O$	15.00	[12]
$Ca(UO_2)_2(SiO_3OH)_2(c) + 6H^+ = 2UO_2^{2+} + Ca^{2+} + 2Si(OH)_4^0$	17.62	[12]

Results of Calculations

Selected results of the simulations are shown in Figures 1–7.

Figure 1 shows profiles of Eh versus radial distance from the center of the source region at various times up to 10^{13} s. The profiles begin at a distance of 0.05 m beyond the boundary between the source region and the spatial domain in which diffusive transport occurs. It is evident that no distinct, moving redox front developed up to 10^{13} s. Instead, a small, gradual increase of Eh occurred near the source boundary. The Eh did not exceed a value of −0.26 v at a distance of 0.05 m from the boundary, which was held at a value of +0.30 v. Identical profiles were obtained with and without precipitation. This was the result of stabilization of the Eh in the domain of transport by diffusion, toward the source region, of reductant at an Eh of −0.36 v, in qualitative agreement with experimental results reported for basaltic and granitic ground waters [4].

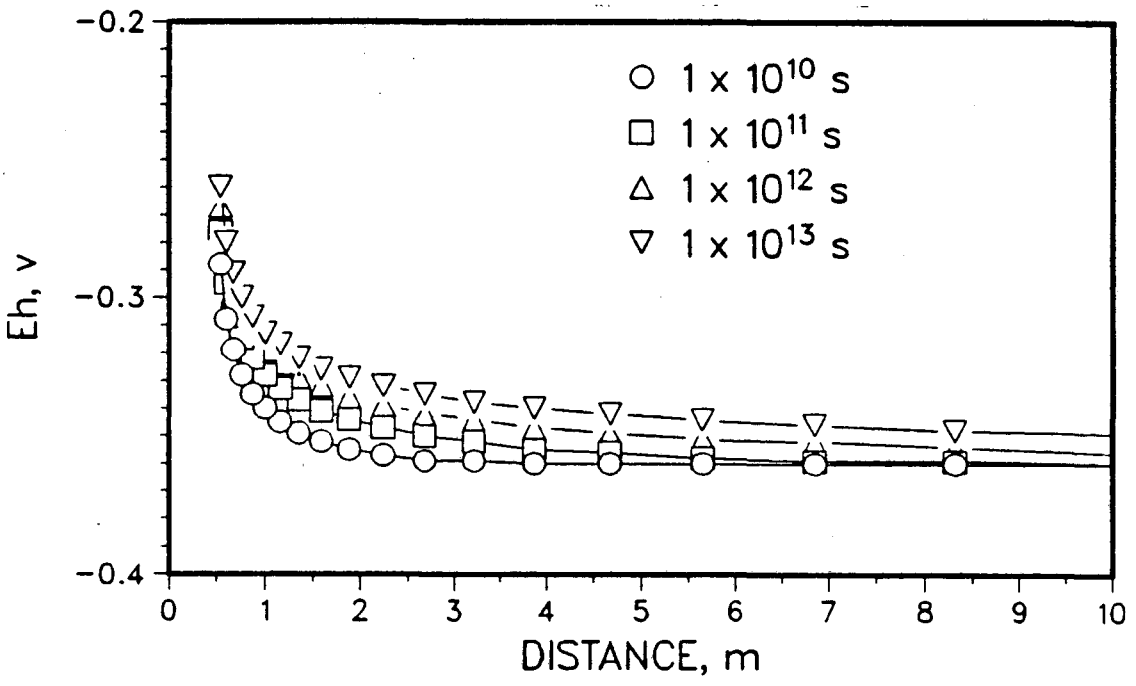

Figure 1. Oxidation potential (Eh) vs. radial distance at simulated times 1×10^{10}, 1×10^{11}, 1×10^{12}, and 1×10^{13} s.

Figure 2 shows profiles of total uranium concentrations in the fluid phase at various times when precipitation of solid phases was excluded from the simulations. Without precipitation, the *total* uranium concentration is unaffected by variations of pH and Eh, although the distribution of *individual species* of uranium is affected. In this case, the total uranium concentration C at time t and distance R in the cylindrical coordinate system is given by the analytical solution [14]:

$$\frac{C}{C_0} = 1 + \frac{2}{\pi}\int_0^\infty \left[\exp\left(-Dtu^2\right)\right]\left[\frac{J_0(Ru)Y_0(R_0u) - Y_0(Ru)J_0(R_0u)}{J_0^2(R_0u) + Y_0^2(R_0u)}\right]\frac{du}{u}, \qquad (1)$$

where C_0 is the constant source concentration at boundary $R = R_0$, D is the diffusion coefficient, and $J_0(x)$ and $Y_0(x)$ are Bessel functions of the first and second kinds of order zero with argument x. Thus, in this case profiles of total uranium concentrations in solution at any time could have been predicted without consideration of homogeneous chemical reactions. However, the results shown in Figure 3 indicate that such predictions

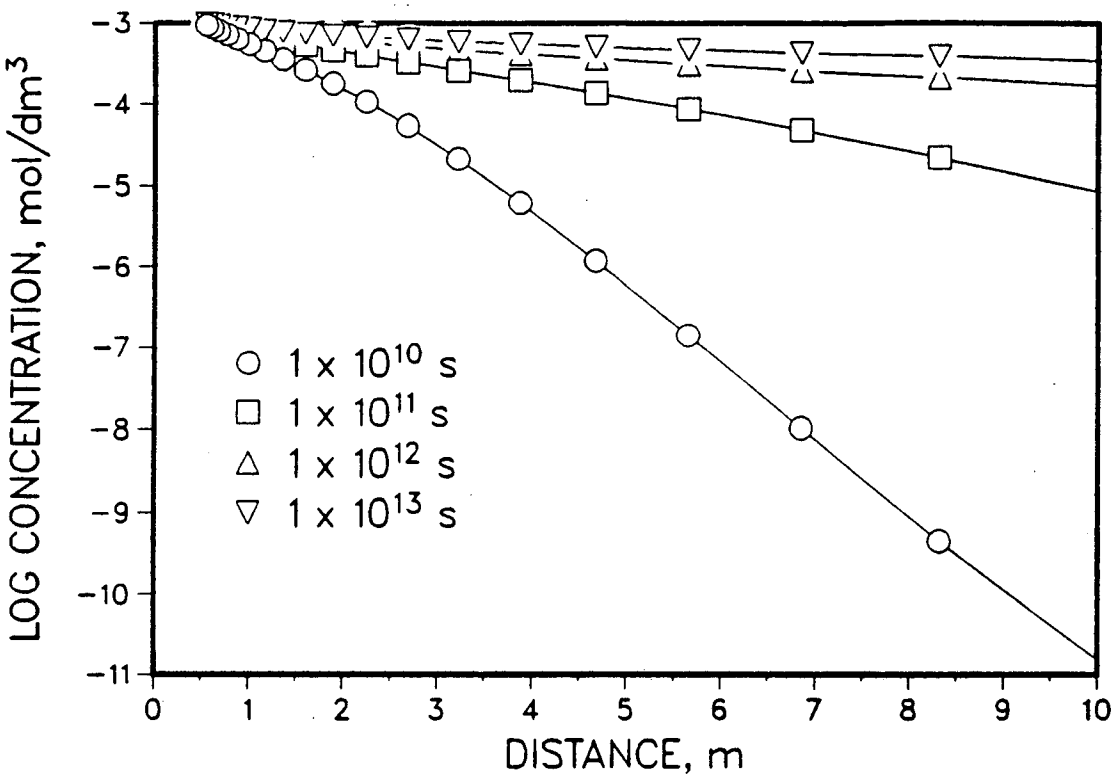

Figure 2. Total uranium concentrations in fluid phase *without* precipitation of solids vs. radial distance at simulated times 1×10^{10}, 1×10^{11}, 1×10^{12}, and 1×10^{13} s.

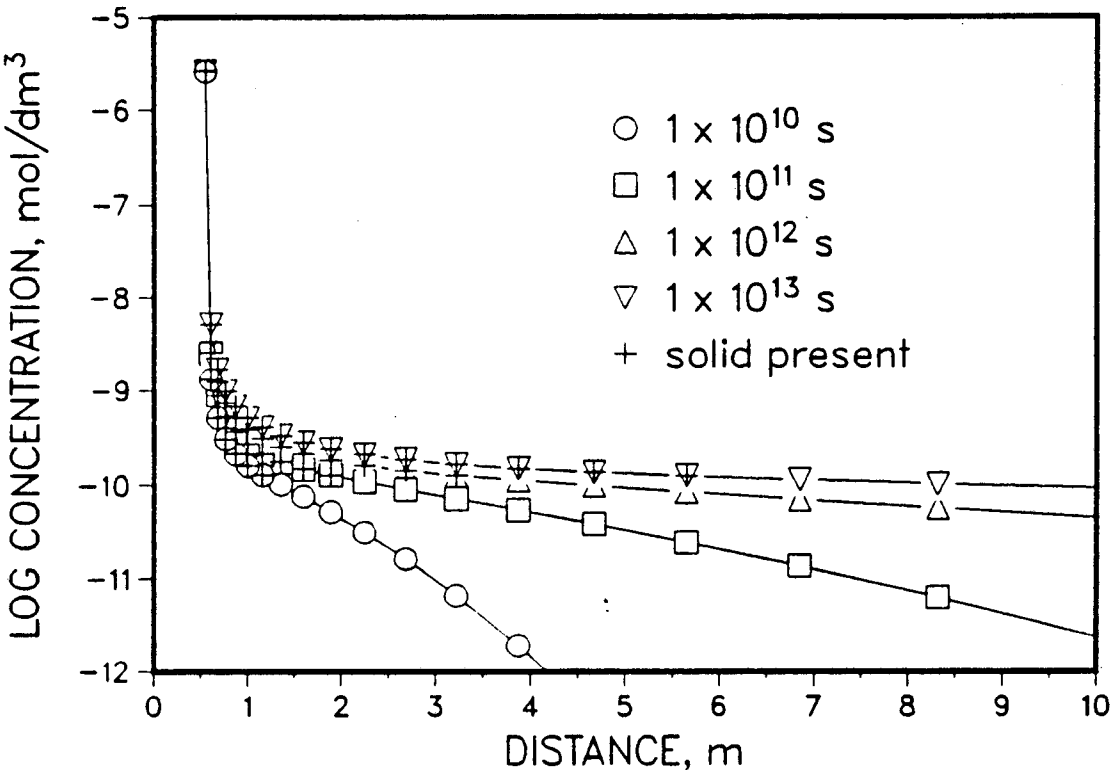

Figure 3. Total uranium concentrations in fluid phase *with* precipitation of solids vs. radial distance at simulated times 1×10^{10}, 1×10^{11}, 1×10^{12}, and 1×10^{13} s.

would be erroneous if the solubility products of certain uranium-containing solids were to be exceeded within the domain of transport.

Figure 3 shows profiles of total uranium concentrations when precipitation of solids was included in the simulations. Although five solids were included, only three (coffinite, uraninite, and calcium uranate) were precipitated in the spatial domain. In Figure 3, finite-difference nodes where solids were present are indicated by superposed crosses. (A detailed plot of the distribution of individual solid phases at 10^{13} s is shown in Figure 6.) Precipitation significantly reduced uranium concentrations in the fluid phase, relative to the case (Figure 2) in which precipitation was not included. The reduction amounted to six to seven orders of magnitude at radial distances greater than a meter from the source boundary. Uranium concentrations in equilibrium with solids were higher (but still reduced by more than two orders) very close to the boundary because of reduced concentrations of Ca^{2+} and $Si(OH)_4^0$ there. The sequence of precipitation at the node closest to the boundary (0.05 m from the boundary) was coffinite at 2.50×10^2 s, uraninite at 3.37×10^6 s, and calcium uranate at 1.25×10^7 s. Thus, inclusion of the possibility of precipitation in these simulations provided a predictive capability beyond the scope of the analytical model given by eq. (1).

Figures 4 and 5 show concentration profiles at 10^{13} s of the uranium solution species $UO_2(CO_3)_2^{2-}$, $(UO_2)_2(OH)_3CO_3^-$, and $U(OH)_4^0$ for simulations without and with precipitation of solids, respectively. In both cases, the profiles are dominated by the uranium(IV) species $U(OH)_4^0$, as expected from the variation of Eh within the domain of transport. In Figure 4, the binuclear complex $(UO_2)_2(OH)_3CO_3^-$ contributes significantly to the total uranium concentration very near the source boundary, causing an observable decrease of concentration of $U(OH)_4^0$ in that region, while the complex $UO_2(CO_3)_2^{2-}$ has a concentra-

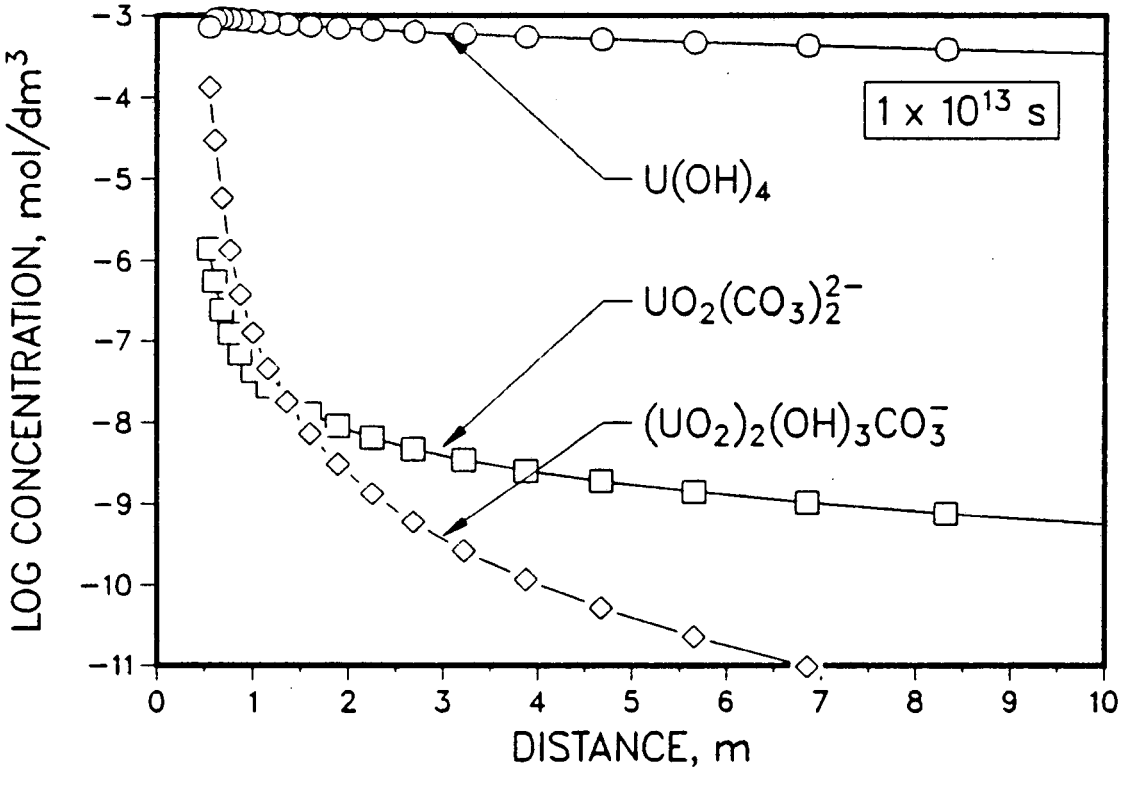

Figure 4. Concentrations of uranium species in fluid phase *without* precipitation of solids vs. radial distance at simulated time 1×10^{13} s.

tion lower by a factor of about 10^2. On the other hand, in Figure 5 concentrations of both $(UO_2)_2(OH)_3CO_3^-$ and $UO_2(CO_3)_2^{2-}$ contribute negligibly to total uranium concentration. The concentration of $U(OH)_4^0$ decreases by more than two orders of magnitude as distance increases slightly from the source boundary. The enhanced concentration of $U(OH)_4^0$ adjacent to the boundary is attributed to the localization of uraninite there; under conditions at that location, uraninite has a higher solubility than either calcium uranate or coffinite, which are not so localized.

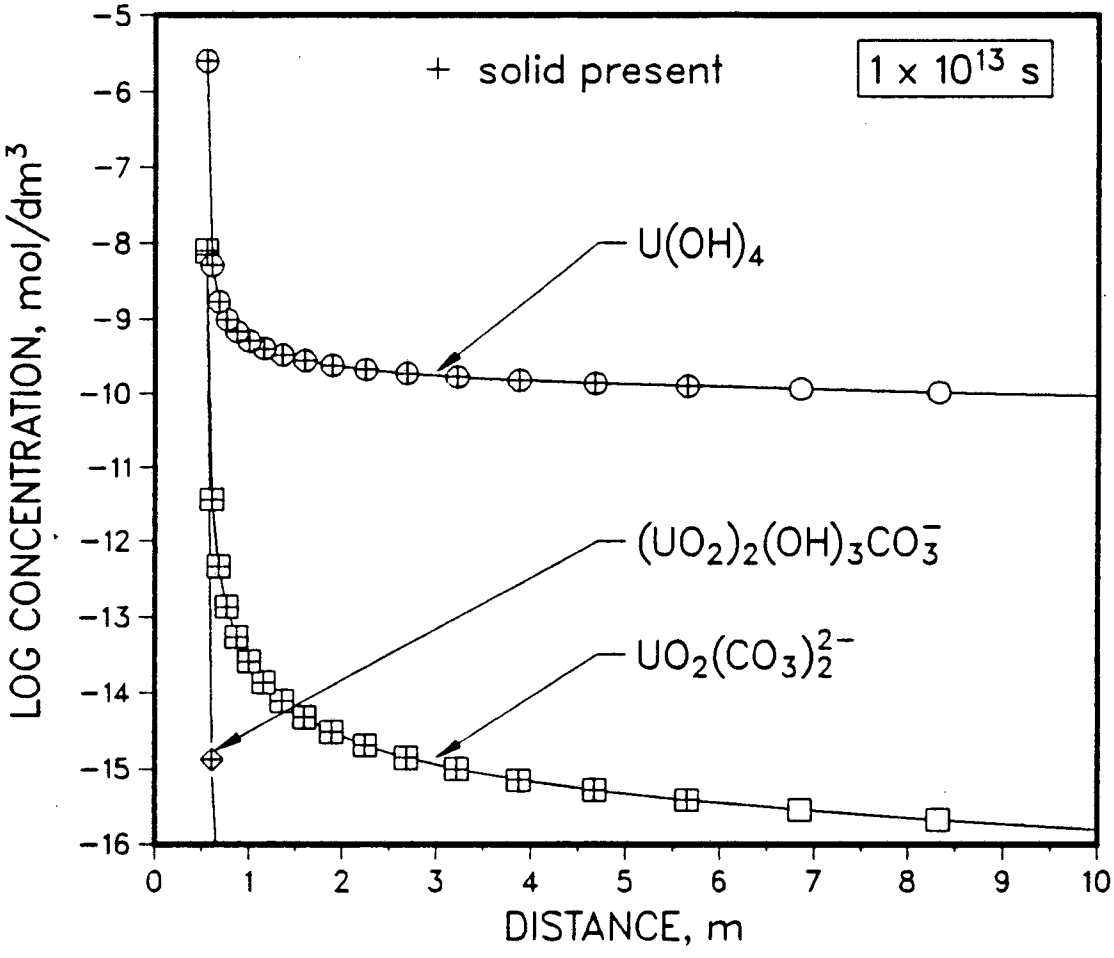

Figure 5. Concentrations of uranium species in fluid phase *with* precipitation of solids vs. radial distance at simulated time 1×10^{13} s.

Figure 6 shows the distribution of solids at 10^{13} s. Here, "concentrations" of solids are expressed as moles of solid per unit volume of fluid phase at each finite-difference node. It is noted that the concentration of uraninite at the node closest to the source boundary was approximately 370 mol/dm^3 at this time; using a specific gravity of 10 for uraninite, this concentration corresponds to approximately 10 dm^3 of uraninite per dm^3 of fluid, or 10 times the available pore space. Computational results at earlier times indicate that complete plugging of the pore space at this node occurred at about 1.0×10^{12} s, when the total solids concentration reached 1 dm^3 of solid per dm^3 of fluid. The non-physical result that precipitation of uraninite exceeds the available pore space at the first spatial node does not affect downstream diffusion of species in local equilibrium with precipitated solids. Precipitation at the first and subsequent nodes fixes concentrations of uranium

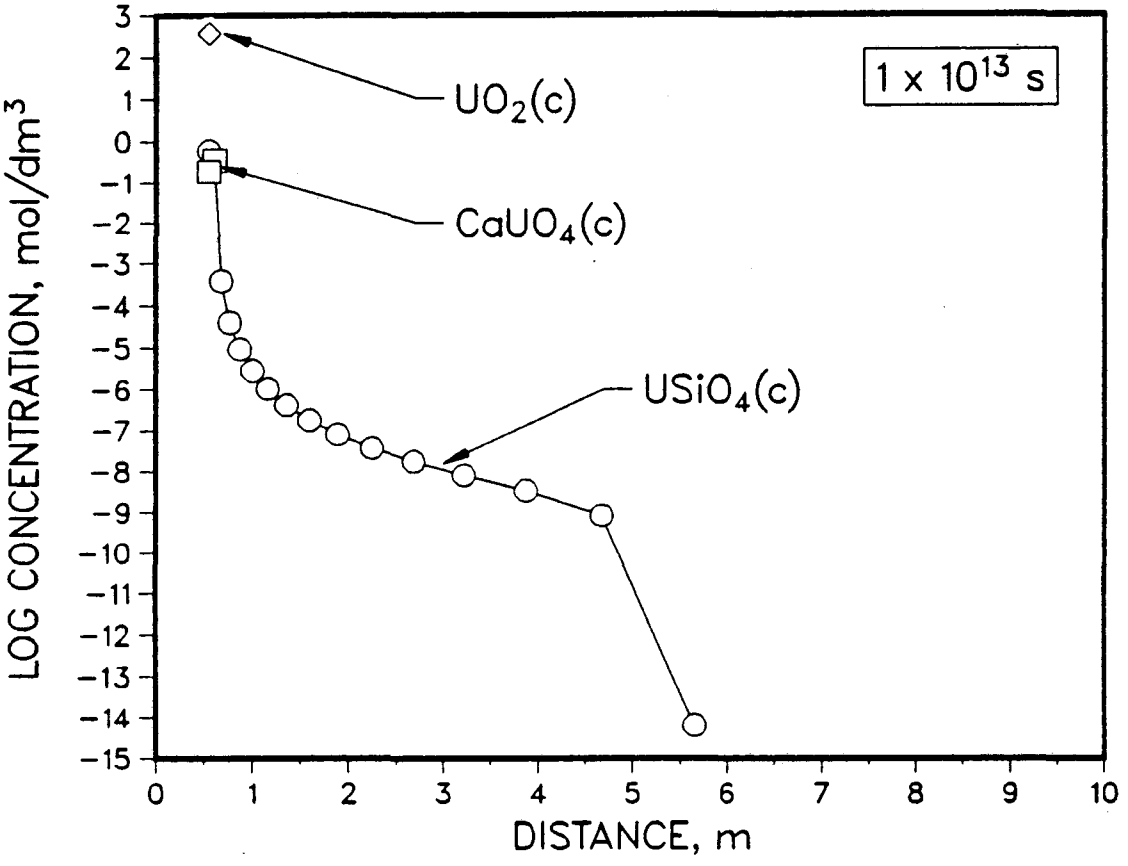

Figure 6. Moles of solids per dm^3 of fluid phase vs. radial distance at simulated time 1×10^{13} s.

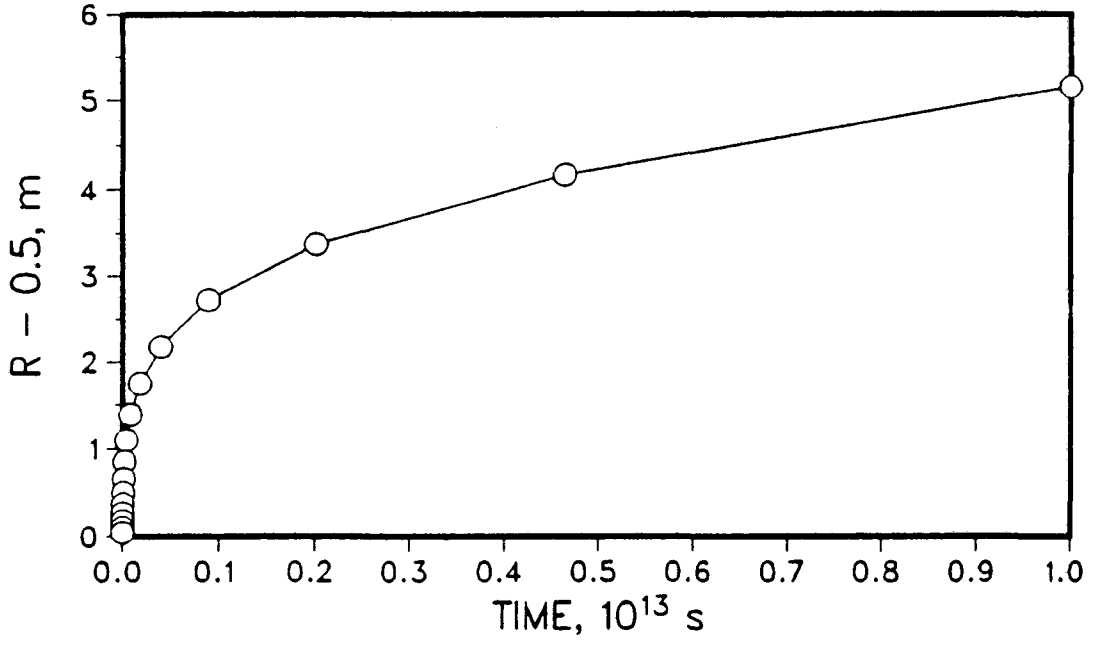

Figure 7. Distance from source boundary ($R_0 = 0.5$ m) where solid coffinite precipitates vs. time of initial precipitation at that distance.

solution species regardless of the quantity of precipitate present. Also in Figure 6 it is seen that migration of coffinite occurred while uraninite and calcium uranate remained localized near the source region. This effect is a consequence of the lower solubility of coffinite and increasing concentration of $Si(OH)_4^0$ as distance from the source boundary increased.

Figure 7 is a graph of the times at which precipitation of coffinite occurred at progressively greater distances from the source boundary, which was located at $R_0 = 0.5$ m in the radial coordinate system. The slope of the curve is the velocity of the leading edge of the zone of solid coffinite, and it is seen that this velocity steadily decreased with time up to the maximum time simulated, 10^{13} s. However, it is noted from Figure 6 that even at this time the bulk of all solids had not migrated from the near vicinity of the source boundary.

SUMMARY AND CONCLUDING REMARKS

The simulations produced the following observations.

- No expanding redox fronts existed at any simulated time up to the maximum time. Eh values in the domain of transport were elevated slightly above their initial value (-0.36 v) for a small distance from the source and tended toward values steady with time.
- In simulations where precipitation of stable solids *was not* allowed, variations of Eh and pH did not affect total uranium concentrations in solution. Concentration profiles could be predicted simply by diffusion of the (constant) source concentrations.
- In simulations where precipitation of stable solids *was* allowed, uraninite and calcium uranate accumulated at the source boundary, while coffinite penetrated further into the spatial domain. Total uranium concentrations in regions of precipitation were determined by solubilities of the precipitated solids, and were six to seven orders of magnitude lower than those in the simulations without precipitation, throughout the spatial domain.

The lack of formation of a moving redox front in a diffusional system agrees qualitatively with experimental evidence [4]. It appears that *advective* flow is required to produce such a front [1,6]; in this case, the front is propagated by physical displacement of the reducing fluid by the oxidizing fluid.

For systems in which the solubility products of stable solid phases are not exceeded by activities of dissolved species, simple (non-chemical) transport models can predict migration of total elemental concentrations. These models fail, however, for systems in which precipitation of stable solids is possible.

ACKNOWLEDGEMENT

This work was supported by the U. S. Department of Energy under Contract No. DE-AC03-76SF00098.

REFERENCES

1. I. Neretnieks, in Scientific Basis for Nuclear Waste Management VII, edited by G.L. McVay (Elsevier Science Publishers, New York, 1984), pp. 1009–1022.
2. D.W. Shoesmith, S. Sunder, L.H. Johnson and M.G. Bailey, in Scientific Basis for Nuclear Waste Management IX, edited by L.O. Werme (Mater. Res. Soc. Proc. 50, Pittsburgh, PA, 1986), pp. 309–316.

3. S. Sunder, D.W. Shoesmith, L.H. Johnson, G.J. Wallace, M.G. Bailey and A.P. Snaglewski, in Scientific Basis for Nuclear Waste Management X, edited by J.K. Bates and W.B. Seefeldt (Mater. Res. Soc. Proc. 84, Pittsburgh, PA, 1987), pp. 103–113.
4. C.M. Jantzen and N.E. Bibler, in Scientific Basis for Nuclear Waste Management IX, edited by L.O. Werme (Mater. Res. Soc. Proc. 50, Pittsburgh, PA, 1986), pp. 219–230.
5. C.M. Jantzen and G.G. Wicks, in Scientific Basis for Nuclear Waste Management VIII, edited by C.M. Jantzen, J.A. Stone and R.C. Ewing (Mater. Res. Soc. Proc. 44, Pittsburgh, PA, 1985), pp. 29–35.
6. C.L. Carnahan, in Scientific Basis for Nuclear Waste Management X, edited by J.K. Bates and W.B. Seefeldt (Mater. Res. Soc. Proc. 84, Pittsburgh, PA, 1987), pp. 713–721.
7. S.L. Phillips, C.A. Phillips, and J. Skeen, Report LBL-14996, Berkeley, CA, 1985.
8. L. Maya, Inorg. Chem. 21, 2895 (1982).
9. J. Bruno, I. Grenthe, and B. Lagerman, in Scientific Basis for Nuclear Waste Management IX, edited by L.O. Werme (Mater. Res. Soc. Proc. 50, Pittsburgh, PA, 1986), pp. 299–308.
10. J. Bruno, D. Ferri, I. Grenthe, and F. Salvatore, Acta Chem. Scand. A40, 428 (1986).
11. D. Langmuir, Geochim. Cosmochim. Acta 42, 547 (1978).
12. M. Schweingruber, NAGRA Tech. Ber. 81-13, Baden, Switzerland, 1981.
13. C.L. Carnahan, presented at Internat. Conf. on Chemistry and Migration Behaviour of Actinides and Fission Products in the Geosphere, Munich, FRG, 1987 (Proceedings to be published in Radiochimica Acta).
14. H.S. Carslaw and J.C. Jaeger, Conduction of Heat in Solids, 2nd ed. (Oxford University Press, London, 1959), p. 335.

LAWRENCE BERKELEY LABORATORY
TECHNICAL INFORMATION DEPARTMENT
UNIVERSITY OF CALIFORNIA
BERKELEY, CALIFORNIA 94720